

Revisiting the notion of independence in asynchronous cellular automata – a study on s-skewed automata

Souvik Roy*, Shlok Shelat^γ Shrey Salvi[†]

School of Engineering and Applied Science, Ahmedabad University, Gujarat, India

*svkr89@gmail.com, souvik.roy@ahduni.edu.in

shlok.s1@ahduni.edu.in

[†]shrey.s2@ahduni.edu.in

In this study, we question the notion of atomicity property in fully asynchronous cellular automata where two neighbouring cells are not allowed to get updated together. In this direction, after breaking the assumption of atomicity property, we introduce the s -skewed asynchronous updating scheme where we allow s number of neighbouring cells to get updated together where $s \in [1, n]$. As a special case, $s = 1$ reports the fully asynchronous update, and $s = n$ shows the traditional synchronous update. Here, we classify the dynamics of elementary cellular automata (ECA) under s -skewed updating scheme following qualitative (i.e., space-time diagram) and quantitative (i.e., density, activity, Kolmogorov-Sinai entropy) experimental approach. According to the results, some ECA rules show strong resistance against this s -skewed perturbation. However, most ECA rules report abrupt phase transition (i.e., discontinuity), continuous phase transition, and class transition dynamics. Next, based on the two-dimensional density surface, we classify the phase transition dynamics of the ECA system. To understand the abrupt phase change in the microscopic view, we further introduce the notion of a correlated s -skewed updating scheme. Moreover, we compare the phase transition dynamics of the s -skewed system with α -asynchronous cellular automata. Apart from the phase transition dynamics, here, the s -skewed system reports a variety of following class transition dynamics: (a) There are situations where a simple locally chaotic rule can show chaotic dynamics with the effect of s -skewed perturbation; (b) Similarly, a chaotic rule is also capable of generating simple periodic or fixed point dynamics with the effect of this s -skewed perturbation.

Keywords: Asynchronous Cellular Automata (ACA); Atomicity property; s-skewed ACA; Phase Transition; Class Transition.

1. Introduction

Traditionally, cellular automata (CA) force all cells to get updated together following the notion of global clock. In the CA system, this notion of global clock indicates centralized control (or “dependency”) which is not very natural. To break this notion of dependency, the CA research community have explored various asynchronous updating schemes which are able to capture the notion of “independence”. In other words, cells of the CA system are updated independently without the presence of global clock in the asynchronous CA (ACA) system. Here, in search of the true meaning of independence, CA research community have introduced the notion of fully asynchronism [Sethi *et al.*, 2016; Roy *et al.*, 2024a], α asynchronism [Bouré *et al.*, 2012], asynchronism in the context of information loss (delay sensitive [Roy, 2019], β and γ asynchronism [Roy, 2024b]) and δ asynchronism [Roy, 2024c].

nism [Bouré et al., 2012]) where the popular are α asynchronous [Bouré et al., 2012] and fully asynchronous [Sethi et al., 2016; Roy et al., 2024a] updating schemes. The work of [Fatès, 2014] contains the survey of different kinds of asynchronous updating schemes.

In detail, in the alpha asynchronous updating scheme, each cell is updated with probability α and not updated with probability $(1-\alpha)$ which captures the notion of uncontrolled phenomenon. On the other hand, fully asynchronous update selects one cell randomly at each time step for an update following a uniform distribution [Sethi et al., 2016; Roy et al., 2024a; Fatès et al., 2006]. After a casual observation, fully asynchronous updating scheme can be viewed as a sequential updating scheme [Fatès, 2014]. However, in other words, two neighbouring cells can not be updated (together) in one step following the fully asynchronous update, also known as the atomicity property [Roy, 2021]. Here, when we select a cell for update, that cell is denoted as *enabled* cell. During the enabled mode, a cell first scans the neighbour's state; hereafter, the cell updates its state following the state transition function. The entire operation, i.e. scanning states of neighbouring cells and updating self state, can be observed as *atomic*. Therefore, in an alternative view, two neighbouring cells can not be in the enabled mode during the same time step. We denote the above property of fully asynchronous updating scheme as *atomicity* property [Roy, 2021]. However, note that, it is possible to enable multiple cells simultaneously (at the same time step) when the cells are not neighbours. For evidence, in three-neighbourhood (self, left, and right) CA system, it is possible to enable half of the cells simultaneously (at most). In fact, the fully asynchronous system is considered as a model of distributed and concurrent systems [Cori et al., 1993] because of the atomicity property. Following this, according to Fatès [Fatès, 2014], fully asynchronism is the most *natural* updating scheme after considering the continuous nature of ‘real’ time. For example, Fig. 4(a) depicts α asynchronous updating scheme where each cell is associated with probability 0.5 for update. Next, Fig. 4(b) shows fully asynchronous update scheme where we select one cell randomly and uniformly at each time step. Finally, Fig. 4(c) reflects the atomicity property where no two neighbouring cells are enabled simultaneously. Note that, this atomicity property does not hold for α asynchronous updating schemes.

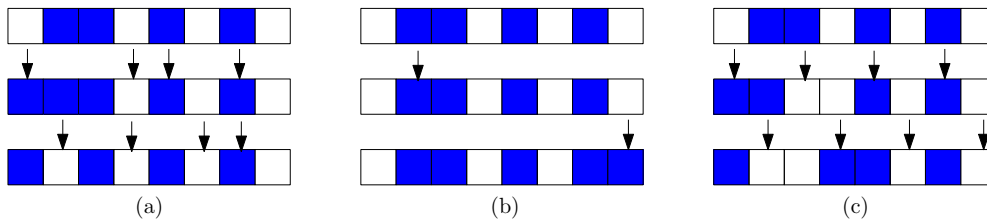


Fig. 1. (a) α asynchronous; (b) fully asynchronous; and (c) atomicity property where colour white and blue respectively represent state 0 and 1. Here, we follow elementary cellular automata 30.

In our early work [Roy et al., 2024b], we question the notion of atomicity property following the below arguments: (a) The notion of atomicity property is not quite natural after considering cellular automata as a model of societal phenomenon. In society, some neighbouring populations follow the same societal norms which violates the independence introduced by atomicity property; (b) Moreover, if we consider cellular automata as a model of natural (physical, biological and chemical) systems, then noise or perturbation in terms of atomicity property is not a good idea. In this context, one can consider the evidence of burst error in network systems. Following this, to break the notion of atomicity property, we have introduced the notion of skewed asynchronous cellular automata where two neighbouring cells are allowed to update together in the same time step. In fact, in the skewed asynchronous updating scheme, we select one cell randomly following uniform distribution, and update the corresponding selected cell and its right (or left) neighbour at each time step. According to the early results [Roy et al., 2024b], some elementary CA rules depict remarkable change in the dynamics with the effect of presence (or absence) of atomicity property. For example, elementary CA rules 26, 58, 90 and 122 respectively show convergent and divergent dynamics after following the fully and skewed asynchronous updating scheme [Roy et al., 2024b]. Similarly, elementary CA rules 38, 54, 134 and 150 show reversible and convergent dynamics under fully and skewed

asynchronous update respectively [Roy *et al.*, 2024b]. In terms of computational ability, Fatès [Fatès, 2024] have pointed out the ability of skewed asynchronous update under 4-neighbourhood dependency in solving parity problem. Note that the same (solution of parity problem) is not true under fully asynchronous update [Fatès, 2024]. Similarly, in our early work [Salvi *et al.*, 2025], we have identified that elementary CA rules 170, 178 and 184 are efficient in solving density classification problem under skewed asynchronous updating schemes.

However, in the skewed asynchronous system, only two neighbouring cells are able to get updated in each time step. That is, here, we restrict the size of the population as two; if the size of the population is more than two, they are not able to follow the same societal norms. In other words, the burst errors are restricted with size two only. Therefore, to generalize the notion of ‘the absence of atomicity property’, here, we introduce the notion of s -skewed updating scheme. In the s -skewed system, we randomly and uniformly select one cell at each time step (say cell i), and update the corresponding selected cell and it’s all $(s-1)$ right neighbouring cells; that is, we update cell $i, i+1, i+2, \dots, i+(s-1)$. Note that, as a special case, $s = 1$ depicts the fully asynchronous system with atomicity property and $s = n$ depicts the classical synchronous cellular automata. In this study, we explore the dynamics of elementary cellular automata (one-dimensional, two-state, three-neighbourhood) rules under s -skewed updating scheme where $s \in [1, n]$. Firstly, we observe the dynamics of ECA rules following the qualitative space-time diagrams following Wolfram’s [Wolfram, 1994] and Li-Packard’s [Li & Packard, 1990] classification. Hereafter, to validate the qualitative results, we follow the quantitative experimental approach (density, activity, and Kolmogorov-Sinai entropy). Here, we ask the following questions to the s -skewed updating scheme: (i) Which rules are able to resist this s -skewed perturbation? (ii) Which rules are capable of depicting (abrupt or continuous) phase transition dynamics for changing value of s -skewed perturbation rate? (iii) Furthermore, we observe the class transition dynamics of the s -skewed system, i.e. for the changing value of s -skewed perturbation rate, the ECA system shows different class dynamics following Wolfram’s [Wolfram, 1994] and Li-Packard’s [Li & Packard, 1990] classification. According to the results, there are some ECA rules which show strong resistance against the s -skewed perturbation; however, there is much evidence of phase and class transition dynamics.

2. Cellular Automata, s -skewed ACA, and Experimental setup

2.1. Cellular Automata and s -skewed ACA

In this study, we consider one-dimensional two-state (i.e., $\{0, 1\}$) three neighbourhood (i.e., self, left, and right) cellular automata under periodic boundary condition, which is popularly known as elementary cellular automata (ECA). Under this periodic boundary ring arrangement, the set of indices that represent each cell is denoted by $\mathcal{L} = \mathbb{Z}/n\mathbb{Z}$ where n denotes the number of cells. At a given time, configuration represents the collection of all states. Therefore, the set of configurations is denoted by $\varepsilon_n = \{0, 1\}^{\mathcal{L}}$. In the elementary cellular system, a cell updates its state following its self state and state of the neighbouring cells (left and right) after considering the local transition function $f : \{0, 1\}^3 \rightarrow \{0, 1\}$. We name the input of local transition function, say (x, y, z) , as *rule mean term* (RMT) r following its decimal equivalent value, i.e., $r = 4 \times x + 2 \times y + z$. Next, we name the eight possible outputs of local transition function as *rule* following its decimal equivalent value, i.e., $f(1, 1, 1) \cdot 2^7 + f(1, 1, 0) \cdot 2^6 + \dots + f(0, 0, 0) \cdot 2^0$. Here, if $f(x, y, z) \neq y$, then the corresponding RMT is denoted as active; otherwise, the RMT is passive. Here, this elementary cellular system is with $2^8 = 256$ rules, where 88 are minimal representative rules and the rest are their equivalent [Li & Packard, 1990].

In the s -skewed updating scheme, we randomly select one cell (say, i) following uniform distribution at each time step. Hereafter, the local rule is applied for update to cell $i, i+1, \dots, i+(s-1)$, i.e., cell i and its $(s-1)$ right neighbours. In other words, starting from the selected cell i , we update consecutive s cells. Let $(U_t)_{t \in \mathbb{N}} \in \mathcal{L}^{\mathbb{N}}$ denotes the random sequence of selected cells. Evolution of the ECA under s -skewed asynchronous updating scheme from an initial configuration x is represented by the stochastic process $(x^t)_{t \in \mathbb{N}}$, and defined recursively by: $x^0 = x$ and $x^{t+1} = F(x^t, U_t)$ with

$$x_i^{t+1} = \begin{cases} f(x_{i-1}^t, x_i^t, x_{i+1}^t) & \text{if } i \in \{U_t, U_t + 1, \dots, U_t + (s - 1)\} \\ x_i^t & \text{otherwise.} \end{cases}$$

Therefore, as special cases, $s = 1$ depicts the fully asynchronous updating scheme [Roy et al., 2024a]; $s = 2$ shows the skewed asynchronous updating scheme [Roy et al., 2024b]; and $s = n$ notes the (traditional) synchronous updating scheme [Wolfram, 1994]. Note that, if $\forall u \in \mathcal{L}, F(x, u) = x$, then a configuration $x \in \varepsilon_n$ is denoted as *point attractor* or *fixed point*.

2.2. Experimental setup

Now, to understand the dynamics of s -skewed asynchronous system, we follow the qualitative and quantitative experimental approaches. Firstly, we need to observe the evolution of the system through space-time diagrams which can be able to provide an important qualitative visual comparison. In our early work [Roy et al., 2024a], we have observed that divisibility of the CA size by k (where, $k \in \{2, 3, 4\}$) plays an important role in the dynamics of fully ACA system ($s = 1$) following the theoretical properties of *primary RMT sets*. Following this, we consider $n \in [40, 50]$ (which, includes divisibility of CA size by k) and evolve the system for 2000 time steps starting from an initial configuration of density 0.5. Moreover, after considering the information flow [Kamilya & Das, 2019] aspect of periodic boundary condition, we validate the result for large CA size $n = 1000$, where we evolve the system for 1000 time steps. In this (initial) qualitative approach, we follow the space-time diagrams of the system to classify it according to Wolfram's [Wolfram, 1994] and Li and Packard's [Li & Packard, 1990] classification. However, note that, this qualitative approach only provides a good visual comparison.

In the formal quantitative approach, we compute the *density*, *activity* and *Kolmogorov-Sinai entropy* of the system during evolution. Here, the density of a configuration c during the evolution of the system at time t can be defined as $d_t = \frac{c_1}{n}$ where c_1 denotes the number of 1 in the configuration c at time t and n denotes the CA size. In this study, we run the system for $T_t = 2000$ time steps, i.e., *transient time*; and compute the average density for (next) $T_s = 100$ time steps, i.e., *sampling time*. Therefore, the average density can be defined as $d = \frac{1}{T_s} \sum_{t=T_t+1}^{t=T_t+T_s} d_t$. Note that, according to the experimental finding of [Fates, 2003], change in sampling time shows a very little impact on the average density after considering $\text{sampling time} \geq n$. Similarly [Fates, 2003], the computed d remains almost same for high *transient time*. However, the same is not true for density of the initial configuration d_0 ($t = 0$). Moreover, the s -skewed perturbation rate s (or, in general, synchrony rate [Fates & Morvan, 2005]) shows large impact on the average density computation. Therefore, the average density of the s -skewed system with perturbation rate s starting from initial density d_0 can be denoted as $d(s, d_0)$. In this computation, the skewed perturbation rate s varies from 1 to n with interval of one; denoted as the set of perturbation rate $S = [0, n](1)$. Similarly, $D_0 = [0.0, 1.0](0.1)$ depicts the set of initial density. Finally, this computation shows a two-dimensional sampling surface for an elementary CA rule. Next, we extract quantitative information from this sampling surface. Firstly, we estimate the effect of small perturbation rate s in the dynamics of the system. Here, *small skewed introduction indicators* are defined by $d_p = \left\{ \frac{1}{|D_0|} \sum_{d_0 \in D_0} [d(1, d_0) - d(2, d_0)]^2 \right\}^{\frac{1}{2}}$

and $d_q = \left\{ \frac{1}{|D_0|} \sum_{d_0 \in D_0} [d(n-1, d_0) - d(n, d_0)]^2 \right\}^{\frac{1}{2}}$. It depicts the “jump” of the system with the effect of small perturbation at the beginning of this synchrony process, i.e., the effect of change in perturbation rate from $s = 1$ to $s = 2$ and $s = n$ to $s = n-1$. Secondly, to estimate the overall change in the global behaviour, *skewed dependence indicator* is denoted by $d_r = \sup_{s \in S_1} \left\{ \frac{1}{|D_0|} \sum_{d_0 \in D_0} [d(s, d_0) - d(s+1, d_0)]^2 \right\}^{\frac{1}{2}}$ where $S_1 = [2, n-2](1)$. Following this quantitative information, we study the properties of the two-dimension sampling surface to classify the s -skewed asynchronous system. In the early work, Fatès et al. [Fates, 2003; Bouré et al., 2011] have argued the limitations of these experimental protocols.

In this study, we also compute the *activity* [Bouré et al., 2011] of the s -skewed system which represents the ratio of *unstable* cell. If a cell changes its state during update (0 to 1, or 1 to 0), then that cell is denoted as unstable. Here, $a_{0 \leftrightarrow 1}$ denotes the number of unstable cells in a configuration c at time t in comparison with the configuration of $(t - 1)$ time. Therefore, $a_t = \frac{a_{0 \leftrightarrow 1}}{n}$ reflects the *activity* of the configuration c at

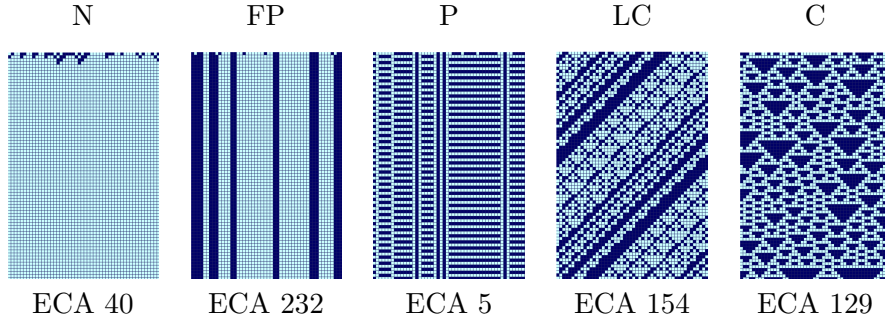


Fig. 2. Evidence of Li-Packard's [Li & Packard, 1990] classification of elementary cellular automata. Here, the CA size is 50, and the system runs for 75 steps. The blue and white box respectively denote state 0 and 1. In the rest part of the text, this convention is kept.

time t . Here, we consider $T_t = 0$ and $T_s = 2000$ to capture the initial instability of the system. Therefore, the *average activity* $a(s, d_0)$ also reflects the two-dimensional sampling surface. Following the same notion of quantitative information, we compute *small skewed introduction indicators* (denoted as a_p and a_q) and *skewed dependence indicator* (denoted as a_r).

Next, we compute the *Kolmogorov-Sinai entropy* [Lei *et al.*, 2021] to capture the uncertainty of the s -skewed asynchronous system. Let us consider, c_0, c_1, \dots, c_t represent the sequence of configurations during the evolution of the system where the system runs for t time steps. Γ_t represents this sequence of configurations. The number of occurrences of (any) configuration $c \in \varepsilon_n$ in the sequence of configurations Γ_t is denoted as Γ_{tc} . Therefore, $\mu(c) = \frac{\Gamma_{tc}}{t+1}$ gives the probability of occurrences of the configuration c in the sequence Γ_t . Now, following the notion of Shannon's entropy, we compute the entropy $H = -\sum_{c \in \varepsilon_n} \mu(c) \log(\mu(c))$ considering the probability space. Therefore, the *entropy* $H(s, d_0)$ also reflects the two-dimensional sampling surface. Following the same notion of quantitative information, we compute *small skewed introduction indicators* (denoted as H_p and H_q) and *skewed dependence indicator* (denoted as H_r). In the experiment, we consider $n = 10$ and run the system for $t = n \times 2^n$ steps. Here, the evolution ($t = n \times 2^n$) provides a fair chance to every configuration. Note that, for large n , it is not possible to follow this experimental setup. However, to validate the entropy results of small CA size ($n = 10$), we also compute the entropy after considering $n = 50$ and $t = 10,000$. It is to be noted that the larger entropy H reflects larger uncertainty of the cellular system, and vice versa. The recent work of [Vispoel *et al.*, 2022] have discussed the limitation of this entropy computation. Finally, in the next sections, we study the s -skewed system following these qualitative (space-time diagram) and quantitative (density, activity and Kolmogorov-Sinai entropy) approaches.

3. Overall qualitative dynamics of s -skewed system

In this section, we first report the qualitative dynamics of s -skewed asynchronous system following the space-time diagram. In this context, according to the space-time diagram of (traditional) ECA system, Wolfram [Wolfram, 1994] has proposed a four class classification. Hereafter, in the similar direction, Li-Packard [Li & Packard, 1990; Martinez, 2013] have proposed following (in details) classification.

- (i) Null class (denoted as N): homogeneous point attractor, i.e., all 0 or all 1, dynamics.
- (ii) Fixed Point class (denoted as FP): inhomogeneous point attractor dynamics.
- (iii) Periodic class (denoted as P)
- (iv) Locally Chaotic class (denoted as LC): chaotic dynamics confined by domain walls.
- (v) Chaotic class (denoted as C).

For example, Fig. 2 depicts the evidence of space-time diagrams following Li-Packard's [Li & Packard, 1990] classification. In this study, we initially follow the Li-Packard's [Li & Packard, 1990] classification to classify the s -skewed system. However, we also consider the situation where Li-Packard's [Li & Packard,

Table 1. Overall classification of s -skewed asynchronous system.

	0	4	8	12	13	14 ($n \in 2\mathbb{N} + 1$)	15 ($n \in 2\mathbb{N} + 1$)	28
Robust	29	32	36	40	44	72	76	77
	78	104	128	132	136	140	142	156
	160	164	168	172	200	204	232	
Discontinuity	2	10	24	34	42	56	74	130
	138	152	154	162	170	184		
Phase Transition	6	18	22 ($n \in 2\mathbb{N}$)	26	38	50	54	58
	90	106	122	134	146	150	178	
Class transition	1	3	5	7	9	11	14 ($n \in 2\mathbb{N}$)	15 ($n \in 2\mathbb{N}$)
	19	22 ($n \in 2\mathbb{N} + 1$)	23	25	27	30	33	35
	37	41	43	45	46	51	57	60
	62	73	94	105	108	129	137	

1990] classification is not able to capture the s -skewed system dynamics, i.e., it is not possible to mark the class of s -skewed system with any of the above mentioned classes. In fact, this study shows this kind of evidence. Here, we denote the class of ECA R with the effect of skewed perturbation rate s as $\mathbb{C}(R, s)$. For example, in Fig. 2, $\mathbb{C}(40, n) = \mathbb{N}$, $\mathbb{C}(232, n) = \text{FP}$, $\mathbb{C}(5, n) = \mathbb{P}$, $\mathbb{C}(154, n) = \text{LC}$, and $\mathbb{C}(129, n) = \mathbb{C}$. Moreover, in this study, we only consider 88 minimal representative elementary CA rules [Li & Packard, 1990]. According to the space-time diagram, we classify the s -skewed asynchronous ECA system into the following four classes.

1. Firstly, there are some ECA rules which show robust dynamics with the effect of s -skewed perturbation. That is, if we progressively change the s -skewed perturbation rate s , the dynamics of the ECA rules remain the same. For example, in Fig. 3, ECA 232 shows FP dynamics under traditional synchronous system ($s = n$). If we introduce s -skewed perturbation, then, the system again shows fixed point dynamics, which is true for any $s \in [1, n - 1]$. In Fig. 3, we report the evidence for $s \in \{1, 2, 10, 25, 40\}$. Therefore, this kind of rule is able to strongly resist the s -skewed perturbation. In Table 1, we note the class of this kind of rules as *robust*. In general, for a $R \in \text{robust}$, $\mathbb{C}(R, s_1) = \mathbb{C}(R, s_2)$ where $s_1, s_2 \in [1, n]$. Out of 88 minimal representative rules, 31 rules belong to this robust class. Note that, ECA 14 and 15 show this robust dynamics when the CA size is not divisible by 2 ($n \in 2\mathbb{N} + 1$).
2. Next, we report the *discontinuity* class where the ECA system shows abrupt phase change after the introduction of a small amount of s -skewed perturbation. According to Table 1, 16 minimal elementary CA rules show this discontinuity dynamics. In this situation, the cellular system shows class dynamics, say X (where $X \in \{\text{FP}, \mathbb{P}, \text{LC}, \mathbb{C}\}$), under synchronous update scheme, i.e. $s = n$. Hereafter, if we introduce a minimal possible small amount of perturbation, the system shows homogeneous point attractor dynamics. That is, the system shows null class dynamics for $s = n - 1$. And, the same holds for increasing value of perturbation rate, i.e. $s \in [1, n - 1]$. In general, for a $R \in \text{discontinuity}$, $\mathbb{C}(R, s) = \mathbb{N}$ where $s \in [1, n - 1]$ and $\mathbb{C}(R, n) = X$ where $X \in \{\text{FP}, \mathbb{P}, \text{LC}, \mathbb{C}\}$. Here, in Fig. 3, ECA 42 depicts this discontinuity dynamics, see the homogeneous all 0 point attractor dynamics for $s \in \{1, 2, 10, 25, 40\}$.
3. Most importantly, some elementary CA rules show phase transition dynamics with the effect of s -skewed perturbation, where the skewed system shows non-zero density before a critical value of perturbation rate, say s_c (i.e., $s \in [s_c, n]$). However, after the critical perturbation rate s_c , the system depicts homogeneous point attractor dynamics (i.e., $s \in [1, s_c - 1]$). In other words, we are able to distinguish the dynamics of the system into two phases (active and inactive). CA researchers have investigated the most to identify the phase transition dynamics in different asynchrony models of cellular automata [Roy et al., 2022; Martínez et al., 2013; Ninagawa et al., 2014]. For example, in Fig. 3, ECA 50 depicts the phase transition dynamics where the system converges to homogeneous point attractor all 0 for $s \in [1, 3]$ and the system shows (kind of) periodic dynamics for $s \in [4, n]$. Here, for evidence, see the space time diagram for $s \in \{1, 2, 10, 25, 40, 50\}$ in Fig. 3. Here, in Table 1, we report the 15 minimal representative rules with phase transition dynamics. Moreover, ECA 22 only shows the phase transition dynamics when the CA size is divisible by 2 (i.e. $n \in 2\mathbb{N}$). In general, we write the following $\mathbb{C}(R, v) = \mathbb{N}$ and $\mathbb{C}(R, u) = X$ where $v \in [1, s_c - 1]$, $u \in [s_c, n]$

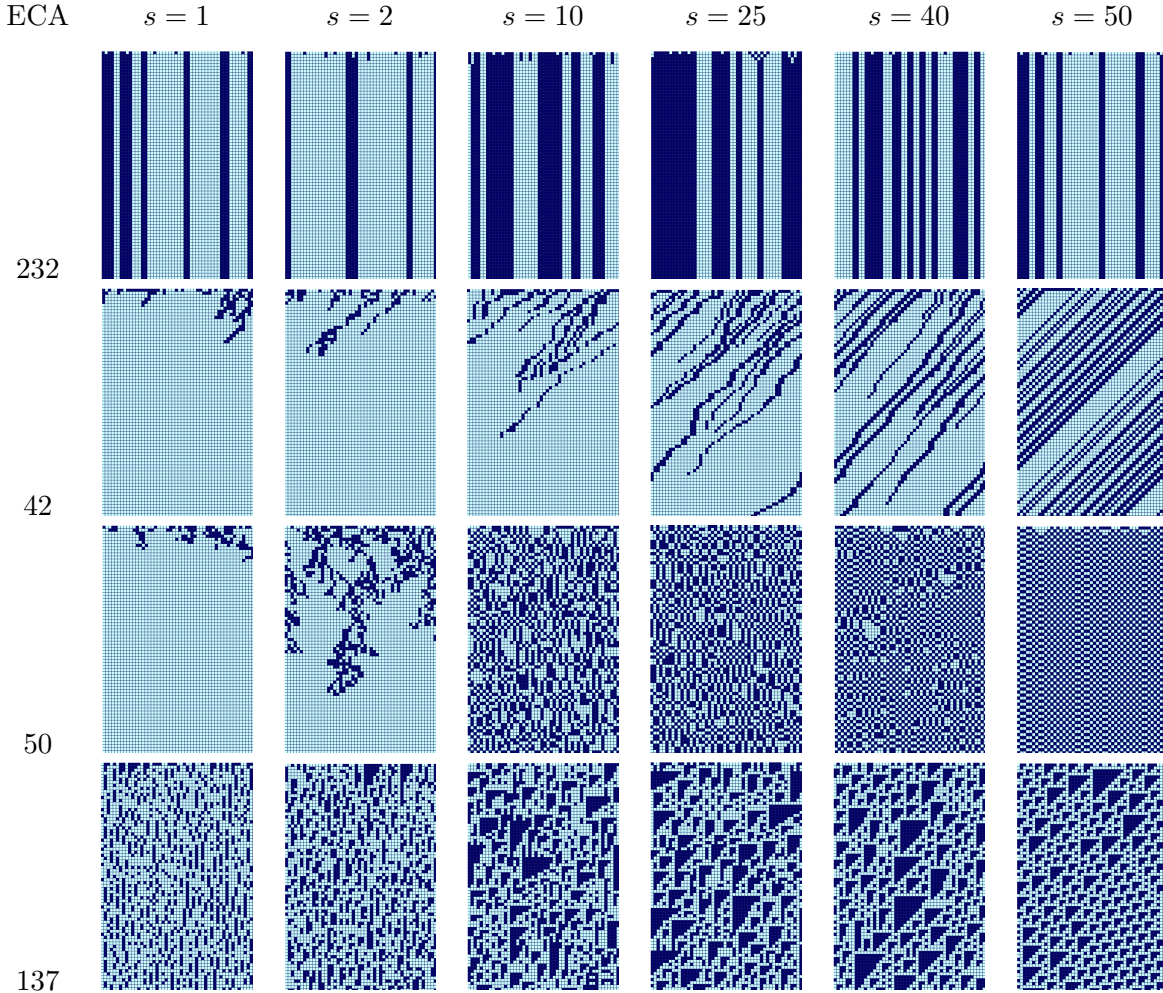


Fig. 3. Overall space-time dynamics under s -skewed updating scheme.

and $X \in \{ \text{FP}, \text{P}, \text{LC}, \text{C} \}$. Note that, in Table 1, there are evidences where the system changes its phase (active \leftrightarrow inactive) multiple time with the progressive change of skewed perturbation rate.

4. Lastly, we discuss the class transition dynamics of s -skewed asynchronous system where the system shows different class dynamics for different skewed perturbation rates. Following this, in the class transition dynamics, the s -skewed system changes the class dynamics after a critical value of perturbation rate, say s_c . That is, $\mathbb{C}(R, u) \neq \mathbb{C}(R, v)$ where $u \in [1, s_c - 1]$ and $v \in [s_c, n]$. Note that, if the s -skewed system changes the class dynamics multiple time for the progressive change in perturbation rate s , then we get multiple critical value. Moreover, one can consider phase transition as a special case of class transition where the system moves towards null class for changing value of perturbation rate. Here, in Fig. 3, ECA 137 depicts the class transition dynamics where $\mathbb{C}(137, 50) = \mathbb{C}(137, 40) = \text{C}$, however, $\mathbb{C}(137, 1)$ and $\mathbb{C}(137, 2)$ depict simple (kind of noisy) dynamics. In Table 1, 31 minimal representative ECA shows class transition dynamics where ECA 14 ($n \in 2\mathbb{N}$), 15 ($n \in 2\mathbb{N}$) and 22 ($n \in 2\mathbb{N} + 1$) show dependency on CA size.

To sum up, in this section, we follow only the space-time diagram to classify the s -skewed asynchronous system in Table 1. In the following sections, we also consider the density, activity, and Kolmogorov-Sinai entropy of the system to validate these results. Moreover, we report the variety of phase and class transition dynamics shown by the s -skewed system with the effect of perturbation in the following sections. Additionally, we introduce the situations where Li-Packard's [Li & Packard, 1990] classification unable to capture the dynamics of s -skewed system.

Table 2. Elementary CA rules with their class of two-dimensional surface which show strong resistance against s -skewed asynchronous perturbation.

Null	$0_{A,A,A}$	$8_{A,A,A}$	$32_{A,A,A}$	$40_{A,A,A}$	$128_{A,A,A}$	$136_{A,A,A}$	$160_{A,A,A}$	$168_{B,A,A}$
Fixed Point	$4_{A,A,A}$	$12_{A,A,A}$	$13_{A,A,A}$	$36_{A,A,A}$	$44_{A,A,A}$	$72_{C,A,A}$	$76_{A,A,A}$	$77_{A,A,A}$
	$78_{A,A,A}$	$104_{C,A,A}$	$132_{A,A,A}$	$140_{A,A,A}$	$164_{A,A,A}$	$172_{D,A,A}$	$200_{A,A,A}$	$204_{A,A,A}$
	$232_{C,A,A}$							
Periodic	$14_{A,A,A} (n \in 2\mathbb{N} + 1)$	$15_{A,A,A} (n \in 2\mathbb{N} + 1)$	$28_{A,A,A}$	$29_{A,A,A}$	$142_{D,A,A}$	$156_{A,A,A}$		

4. Quantitative dynamics of s -skewed system

In this section, we revisit the dynamics of the s -skewed asynchronous system following both the qualitative and quantitative approach. Recall that, here, we consider density, activity, and Kolmogorov-Sinai entropy in the quantitative study. First, we compute the two-dimensional sampling surface after considering average density (denoted as ‘ d ’), average activity (denoted as ‘ a ’), and entropy (denoted as ‘ H ’) for changing initial density $d_0 \in D_0$ and skewed perturbation $s \in S$. Hereafter, to extract the quantitative information of the two-dimensional sampling surface, we compute the *small skewed introduction indicator* (say, for two-dimensional average density surface) d_p and d_q and *skewed dependence indicator* d_r . Based on these quantitative information (i.e., d_p , d_q , and d_r), we classify the two-dimensional surface. During the classification, if any of the *small skewed introduction indicator* (either d_p or d_q) is big, we consider the overall *small skewed introduction indicator* is big. On the other hand, if both of the *small skewed introduction indicator* (d_p and d_q) are small, we consider the overall *small skewed introduction indicator* is small. Therefore, following are the proposed four classes:

Class A: small d_p , small d_q , and small d_r (i.e., *small skewed introduction indicator* is small and *skewed dependence indicator* is small).

Class B: either d_p or d_q is big, and d_r is small (i.e., *small skewed introduction indicator* is big and *skewed dependence indicator* is small).

Class C: small d_p , small d_q , and big d_r (i.e., *small skewed introduction indicator* is small and *skewed dependence indicator* is big).

Class D: either d_p or d_q is big, and d_r is big (i.e., *small skewed introduction indicator* is big and *skewed dependence indicator* is big).

Recall that, the average density $d \in [0, 1]$; therefore, $d_p, d_q, d_r \in [0, 1]$. Here, *small* depicts $d_p \leq 0.1$, and *big* reports the remaining situation. The same is also true for d_q and d_r . Following the similar direction, we also classify the two-dimensional surface of average activity and entropy into four classes. Next, we revisit the *robust* class of Table 1 in details.

4.1. Dynamics of Robust class

In this section, we discuss the dynamics of *robust* class where the system shows strong resistance against the s -skewed asynchronous perturbation. That is, if we progressively change the skewed perturbation rate s , then the system follows same class dynamics. Recall that, for the reference of synchronous dynamics, we consider Li-Packard’s [Li & Packard, 1990] classification, i.e., $\mathbb{C}(R, n) = X$, where $X \in \{\text{N, FP, P, LC, C}\}$. Moreover, for the *robust* class, we know that $\mathbb{C}(R, s_1) = \mathbb{C}(R, s_2)$, where $s_1, s_2 \in [1, n]$ and $R \in \text{robust}$. Therefore, it is possible to conclude that Li-Packard’s classification is completely able to capture the dynamics of the *robust* class, i.e., $\mathbb{C}(R, s) = X$, where $X \in \{\text{N, FP, P, LC, C}\}$ and $s \in [1, n]$. Here, Table 2 depicts 31 robust ECA rules, out of 88 minimal rules, along with their class of two-dimensional surfaces. In Table 2, the classes of the two-dimensional surface are marked with ECA rules following the order – density, activity and entropy. For example, $R_{A,D,B}$ indicates that the two-dimensional density, activity and entropy surface respectively show class A , D and B . In the rest of this paper, we follow this convention. Now, according to the Table 2, following are the possibilities.

1. All the eight *null* ECA rules show strong resistance against s -skewed perturbation. Fig. 4(a) depicts the sample space-time diagram for ECA 40 where $\mathbb{C}(40, s) = \text{N}$ for $s \in [1, n]$; for evidence see the space-time

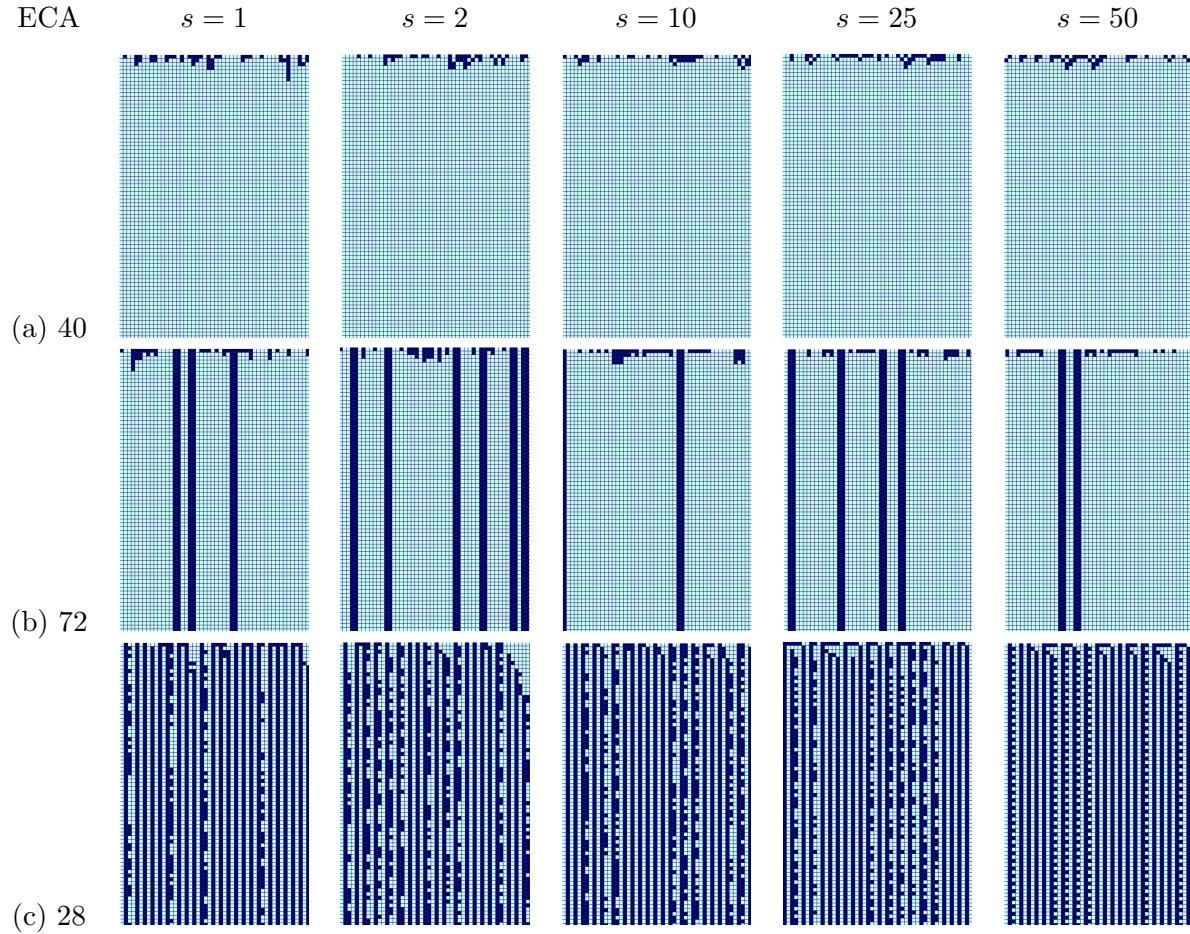


Fig. 4. Space-time dynamics of ECA rules which show strong resistance against s -skewed asynchronous perturbation.

diagram for perturbation rate $s \in \{1, 2, 10, 25, 50\}$. Observe that, in Table 2, two-dimensional surfaces for these rules show class A dynamics which validates their robust dynamics. For evidence, Fig. 5(a), (b), (c) depict the two-dimensional “flat surface” for ECA 40 after considering density, activity and entropy surface respectively. As an exception, two-dimensional density surface for ECA 168 shows class B dynamics which indicates high small skewed introduction indicator. For clarification, Fig. 5(g) depicts the corresponding two-dimensional surface for ECA 168 where the system moves to homogeneous point attractor all 1 starting from initial density $d_0 = 0.9$ (note that, active $101 \rightarrow 1$ and passive $111 \rightarrow 1$ are responsible). However, the null class dynamics of ECA 168 remains same. Here, we report the density surface of ECA 168 as “flat surface with d_0 dependent exceptions”.

2. Next, there are 17 fixed point ECA rules which show robust dynamics under s -skewed asynchronous update, see Table 2. For evidence, Fig. 4(b) reflects the FP dynamics of ECA 72 (i.e., $\mathbb{C}(72, s) = \text{FP}$) for $s \in [1, n]$; see the space-time diagrams in Fig. 4(b) for $s \in \{1, 2, 10, 25, 50\}$. Here again, the two-dimensional sampling surface of these ECA rules in Table 2 depict flat surface or class A dynamics for activity and entropy computation. However, the two-dimensional density surface shows following two kind of dynamics: for some ECA rules, it shows obvious flat surface dynamics; however, for some ECA rules, it shows d_0 -dependent, s -invariant surface. For example, Fig. 5(h), (i) depict the d_0 -dependent, s -invariant density surface for ECA 204 and 232. For example, in the case of ECA 204, if we progressively change the initial density d_0 , then the average density in the two-dimensional surface progressively changes, see Fig. 5(h); therefore, the two dimensional density surface of ECA 204 shows class A, see Table 2. However, the same is not true for ECA 232 (Fig. 5(i)) where the d_0 -dependent sampling surface shows uneven changes (i.e., class C in Table 2).
3. Lastly, 6 periodic elementary CA rules show robust dynamics. For example, Fig. 4(c) depicts the periodic

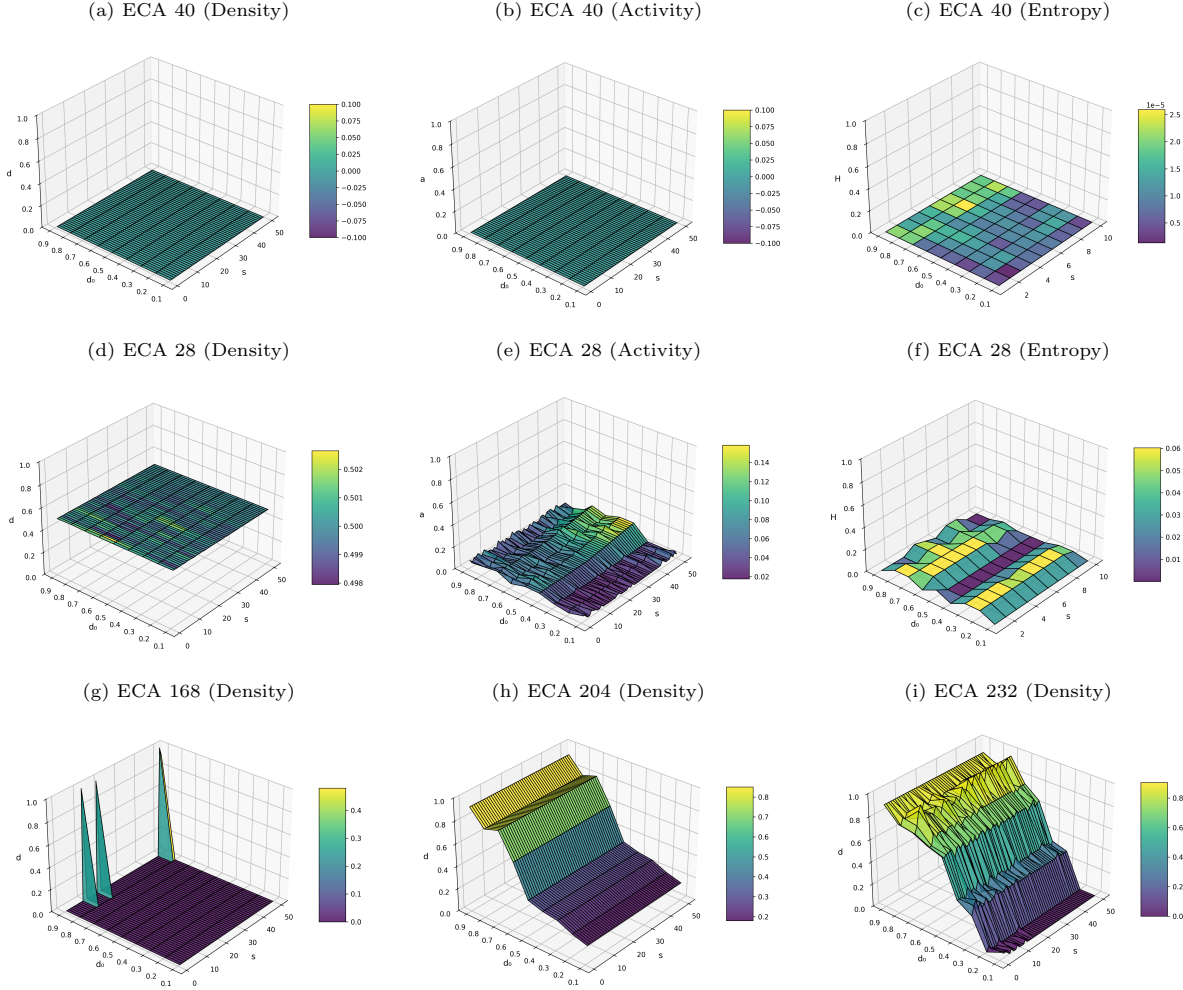


Fig. 5. Two-dimensional surface of ECA rules which show strong resistance against s -skewed asynchronous perturbation.

space-time diagram for ECA 28 with the effect of perturbation s where $s \in \{1, 2, 10, 25\}$. Observe that, in Fig. 4(c), ECA 28 moves from uniform periodic structure to non-uniform periodic structure with the effect of s -skewed perturbation. Here again, the two-dimensional surfaces for activity and entropy remain in class A, see Table 2. Fig. 5(d), (e), (f) reflect the two-dimensional surface for periodic ECA 28 after considering density, activity, and entropy parameter respectively. Here, the two-dimensional sampling surface of periodic rules are not “exactly” flat because of the non-uniform periodic structure. That is, the non-uniform periodic structure changes dependent on the perturbation rate. However, the surface remains “almost” flat, see Fig. 5(e), (f). Note that, in Table 2, ECA 14 and 15 only show robust class dynamics, when the CA size n is not divisible by 2.

Overall, here, ECA rules form the class N, FP, and P show robust dynamics. Therefore, the ECA rules with chaotic and locally chaotic dynamics are not able to show resistance against the s -skewed asynchronous perturbation. According to the quantitative information, the activity and entropy surface show class A (*flat surface*) dynamics for these robust rules. However, the two-dimensional density surface for these robust rules show following dynamics: *flat surface*; *flat surface with d_0 dependent exceptions*; and *d_0 -dependent, s -invariant surface*. However, observe that, initial density d_0 is only responsible for these different density surfaces for different robust rules. The s -skewed perturbation rate is not responsible for this. To sum up, these quantitative results validate the initial space-time dynamics.

Table 3. ECA rules of discontinuity class along with their class of two-dimensional surface under s -skewed updating scheme.

Fixed Point	$2_{B,B,A}$ $152_{B,B,A}$	$10_{B,B,A}$ $162_{B,B,A}$	$24_{B,B,A}$ $170_{D,B,A}$	$34_{B,B,A}$ $184_{D,B,A}$	$42_{B,B,A}$	$56_{B,B,A}$	$130_{B,B,A}$	$138_{D,B,A}$
Locally Chaotic								
Periodic	$154_{B,B,B}$	$74_{B,B,A}$						

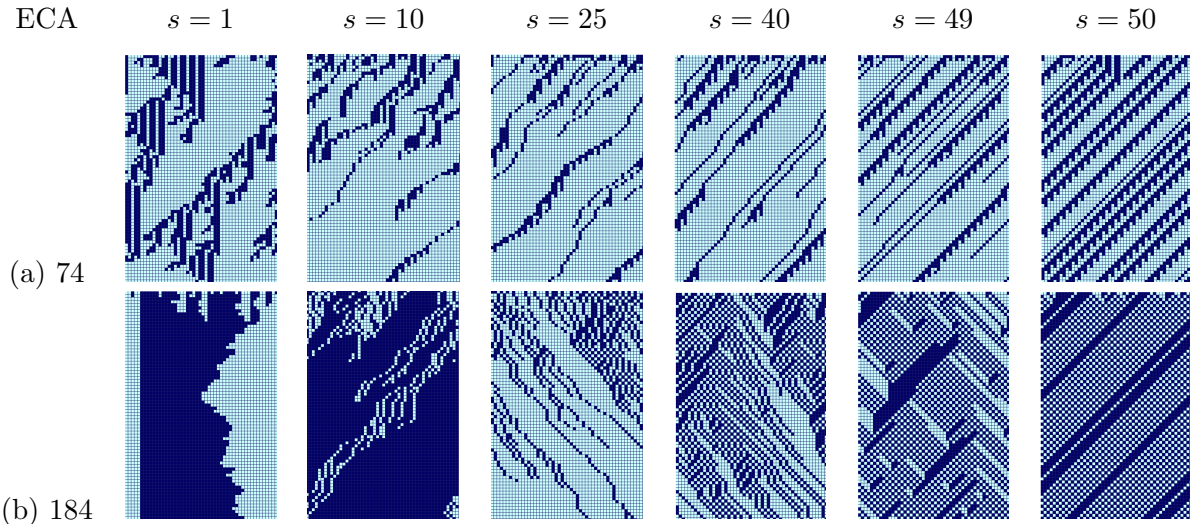


Fig. 6. Discontinuity dynamics under s -skewed updating scheme after considering (a) ECA 74 and (b) ECA 184.

4.2. Dynamics of Discontinuity class

In this section, we discuss the *discontinuity* dynamics of s -skewed system where the system shows abrupt *phase transition* with the effect of small skewed perturbation. That is, $\mathbb{C}(R, n) = \mathbb{X}$ and $\mathbb{C}(R, s) = \mathbb{N}$, where $\mathbb{X} \in \{ \text{FP, P, LC, C} \}$, $s \in [1, n - 1]$ and $R \in \text{discontinuity}$. Therefore, the journey of the skewed system from $s = n$ to $s = n - 1$ show massive change in the dynamics of the system. Here, Table 3 reports the 16 minimal ECA rules of discontinuity class along with their class of two-dimensional sampling surface. Note that, in Table 3, none of the chaotic rules depict this discontinuity dynamics. Following are the observations on the two-dimensional surfaces:

1. Here, most of the ECA rules from the discontinuity class show “*discontinuity surface at $s_c = n$ and flatness for the rest surface*” for density and activity parameter. This surface indicates towards class *B* dynamics. For example, Fig. 7(a), (b) respectively depict the two-dimensional density and activity surface for ECA 74. For the qualitative evidence, Fig. 6(a) depicts the space-time diagram of ECA 74 for $s \in \{1, 10, 25, 40, 49, 50\}$. Observe that, two-dimensional entropy surface also depict the similar surface, however, the H_q indicator remains small, see Fig. 7(c) for ECA 74. Therefore, the two-dimensional entropy surface remains in class *A*. The same is also true for rest of the ECA rules of this discontinuity class. As an exception, ECA 154 moves from locally chaos to null, which reports entropy class *B*.
2. On the other hand, some ECA rules of *discontinuity* class (specifically, ECA 138, 170, 184) depict class *D* dynamics for two-dimensional density surface. For example, Fig. 7(d) reports the two-dimensional density surface for ECA 184 which shows “*unstable surface*”. The same is also true for ECA 138 and 170. Fig. 6(b) depicts the space-time diagram for ECA 184 after considering $s \in \{1, 10, 25, 40, 49, 50\}$. Observe that (in Fig. 6(b)), ECA 184 moves to all 0 point attractor for $s = 25$, however, the skewed system converges to all 1 point attractor for $s = 10$. Here, ECA 184 is associated with two point attractors - all 0 and all 1. Depending on the update sequence U , the system moves to any of these point attractors. According to the qualitative observation, starting from the same initial configuration, the system may converge to

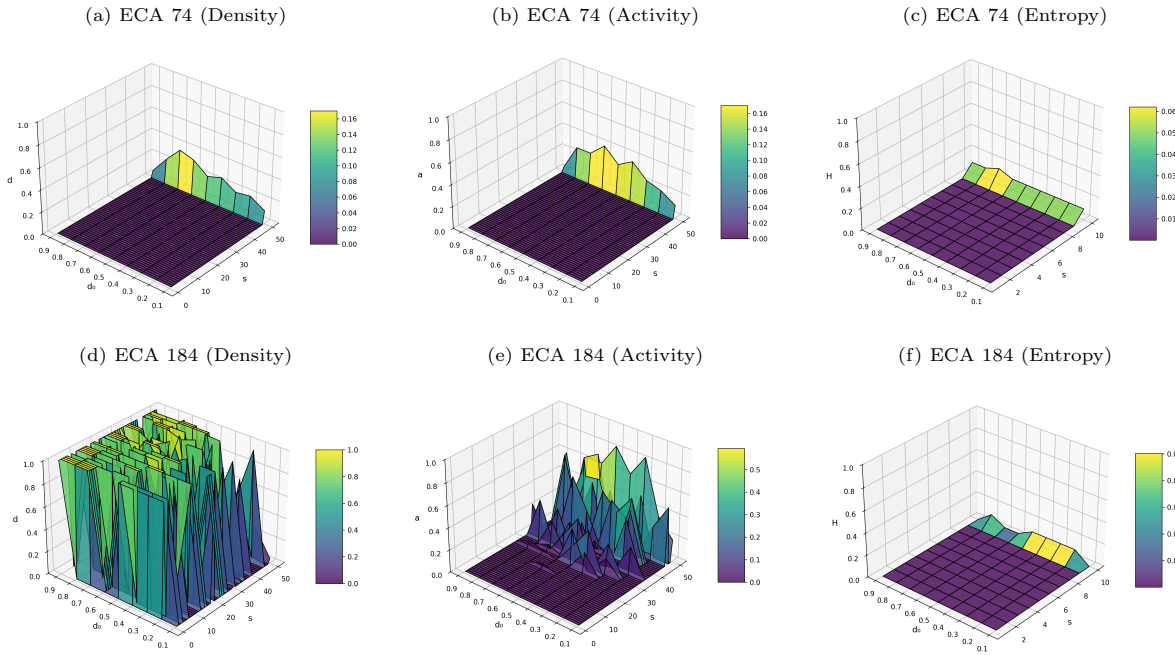


Fig. 7. Two-dimensional density, activity and entropy surface for discontinuity class ECA rules 74 and 184. Here, (a), (b), (c), (f) show *discontinuity surface at $s_c = n$* and *flatness for the rest surface*; and, (d), (e) depict *unstable surface*.

different point attractor for different update sequence U . Therefore, it shows the *unstable surface*. However, for both of the situations (convergence towards all 0 or all 1 point attractor), the system shows N class dynamics. Moreover, the two-dimensional activity surface reflects that the system takes less convergent time for decreasing value of perturbation rate s , see Fig. 7(e). In this context, Fatès [Fatès *et al.*, 2006] have identified that the convergent time for ECA 184 is $\theta(n^3)$ under fully asynchronous update ($s = 1$) following the theoretical probabilistic analysis. Now, if we increase s (say $s = n - 1$), it takes exponential convergent time which is not possible to validate by using the existing experimental setup. Therefore, we validate this discontinuity dynamics for small CA size. This situation also reflects the limitation of this experimental protocol.

To sum up, the ECA rules of discontinuity class show *discontinuity surface at $s_c = n$* and *flatness for the rest surface* or class B dynamics for two-dimensional density and activity surface. However, depending on the number point attractors, the system is also capable to reflect *unstable surface* or class D dynamics. However, the entropy of the system remains stable after introducing the s -skewed perturbation.

4.3. Phase transition Dynamics of s -skewed system

Here, we discuss the *phase transition* dynamics of s -skewed system where the system moves from non-zero density (active phase) to zero density (inactive phase) after a critical value of perturbation rate, say s_c . Therefore, $\mathbb{C}(R, s_1) \neq \mathbb{C}(R, s_2)$ where $R \in \text{phase transition}$, $s_1 \in [1, s_c - 1]$, $s_2 \in [s_c, n]$, and either $\mathbb{C}(R, s_1) = \text{N}$ or $\mathbb{C}(R, s_2) = \text{N}$. Note that, it may also possible that the system moves from active to inactive phase multiple times for changing perturbation rate $s \in [1, n]$. Then, we get multiple critical value for phase transition. Moreover, the study of two-dimensional density surface is enough to identify the phase transition dynamics. Table 4 reports the 15 minimal representative rules of phase transition class along with their class of two-dimensional surface. Here, the s -skewed system shows following variety of phase transition dynamics.

1. First, we discuss ECA 18, where the two-dimensional density surface reflects a *surface with phase transition for $2 > s_c < n$* . Here, in Fig. 8, observe that, the system shows chaotic dynamics for $s = n = 50$; hereafter,

Table 4. ECA rules of phase transition class along with their class of two-dimensional surface under s -skewed updating scheme.

$6_{B,B,A}$	$18_{C,C,C}$	$22_{D,D,A} (n \in 2\mathbb{N})$	$26_{B,B,D}$	$38_{B,B,B}$	$50_{C,C,B}$	$54_{D,B,B}$	$58_{B,B,B}$	$90_{B,B,D}$
$106_{C,C,B}$	$122_{B,B,B}$	$134_{B,B,B}$	$146_{C,C,A}$	$150_{D,D,D}$	$178_{C,C,A}$			

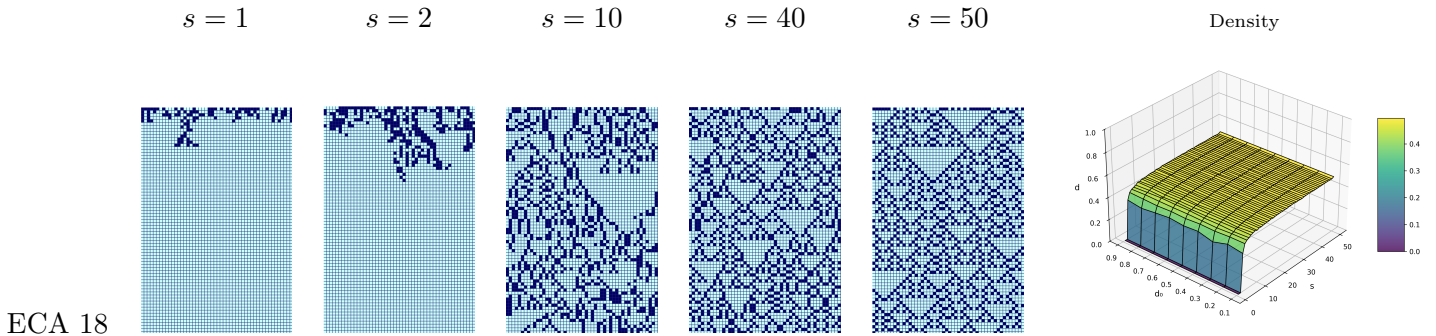


Fig. 8. Phase transition dynamics of ECA 18 under s -skewed updating scheme. Here, ECA 18 depicts a *surface with phase transition for $2 > s_c < n$* (density surface).

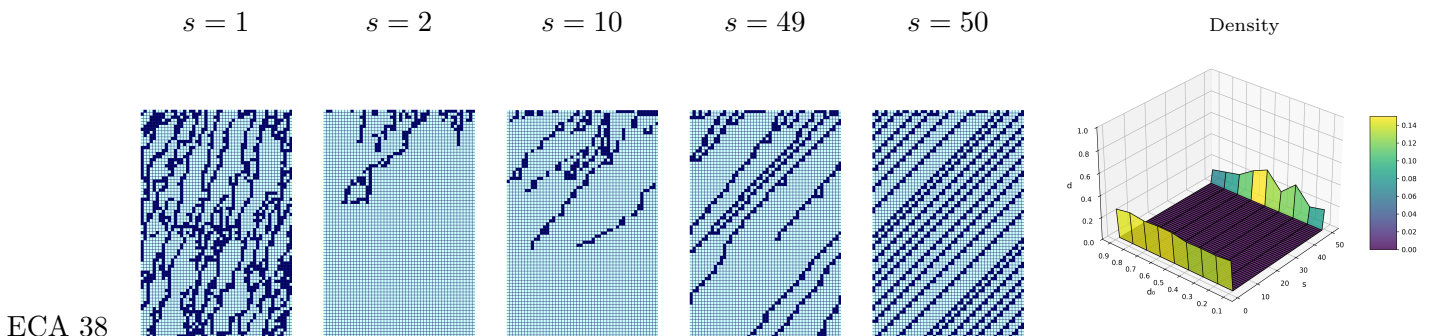


Fig. 9. Phase transition dynamics of ECA 38 under s -skewed updating scheme. Here, ECA 38 shows a \sqcup *surface with phase transition for $s_c = 2$ and $s_c = n$* (density surface).

for $s = 10, 40$; it again shows a chaotic dynamics with noise; next, the skewed system shows inactive \mathbb{N} dynamics for $s = 1, 2$ (specifically, $s_c = 4$). For the quantitative information, see the two-dimensional density surface in Fig. 8. In the quantitative surface, d_p and d_q are small, and, d_r is big, i.e. class C . In the literature, α asynchronous [Bouré *et al.*, 2012] and delay sensitive [Roy, 2019] updating schemes also report this kind of phase transition dynamics. According to [Bouré *et al.*, 2012], these phase transition dynamics are part of the *directed percolation universality class*. Here, according to Table 4, ECA 50, 106, 146 and 178 also depict similar phase transition dynamics. Note that, here, we mark the phase transition for critical value $s_c = 2$ with special attention to understand the importance of atomicity property.

2. Next, we discuss the situation where the s -skewed system shows phase transition for both $s = 2$ and $s = n$. Here, Fig. 9 depicts the space-time diagram of ECA 38 where the cellular system shows active phase for $s = 1$ and $s = n = 50$. However, ECA 38 depicts the \mathbb{N} class dynamics for $s \in [2, n - 1]$; for evidence, see Fig. 9 for $s \in \{2, 10, 49\}$. Here, the two-dimensional density surface reflects a “ \sqcup *surface with phase transition for $s_c = 2$ and $s_c = n$* ”, see Fig. 9. Observe that, here, the quantitative indicators d_p and d_q are big and d_r is small; therefore, the density surface shows class B dynamics. The same is also true for activity surface. According to Table 4, ECA 6 and 134 also depict similar phase transition dynamics. Note that, the atomicity property is responsible for phase transition with critical value $s_c = 2$. However, here, the system shows a abrupt phase transition dynamics. To understand this abrupt change,

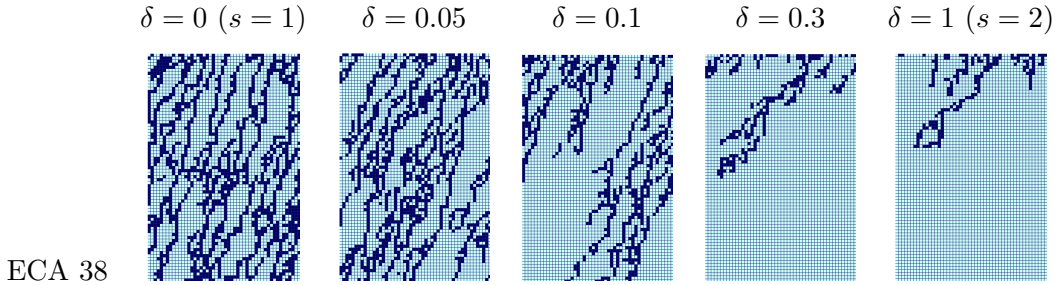


Fig. 10. Phase transition dynamics of ECA 38 under correlated s -skewed ($s = 2$) updating scheme.

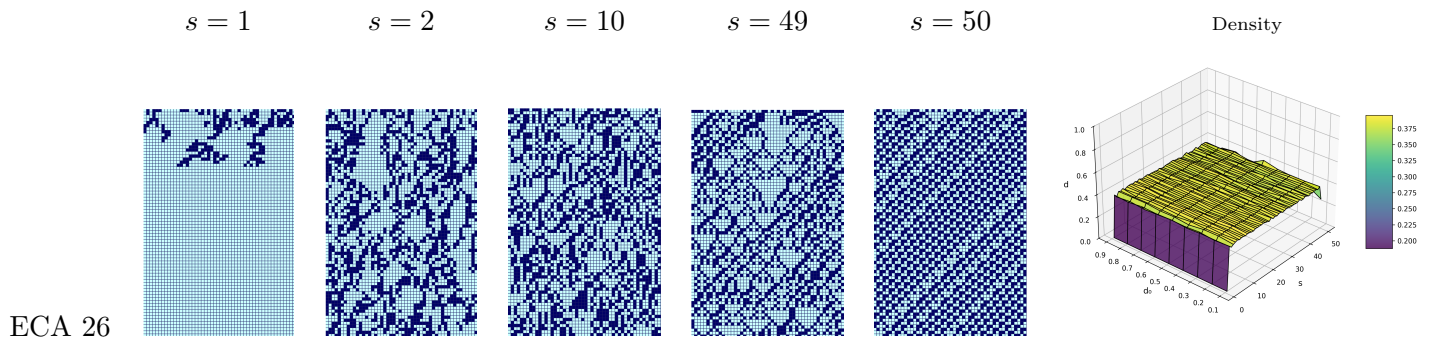


Fig. 11. Phase transition dynamics of ECA 26 under s -skewed updating scheme. Here, ECA 26 depicts density *surface with phase transition for $s_c = 2$* .

here, we study the dynamics of the system following *correlated s -skewed* updating scheme. Recall that, in the $s = 2$ skewed updating scheme, we randomly select one cell (say, i) following uniform distribution at each time step. Hereafter, the local rule is applied for update to cell i and $i + 1$, i.e., cell i and its right neighbour. Now, in the proposed *correlated s -skewed* updating scheme (specifically, $s = 2$), we randomly select one cell (say, i) following uniform distribution at each time step. Hereafter, the local rule is applied for update to cell i (with probability 1), and the local rule is applied for update to cell $i + 1$ with probability δ . That is, for $\delta = 0$, the *correlated s -skewed* system ($s = 2$) shows the dynamics of fully asynchronous system; however, for $\delta = 1$, the system shows the dynamics of $s = 2$ skewed updating scheme.

For example, Fig. 10 depicts the dynamics of ECA 38 for correlated s -skewed ($s = 2$) updating scheme after considering $\delta \in \{0, 0.05, 0.1, 0.3, 1\}$. Here, for $\delta = 0$, i.e., $s = 1$, the system shows active phase; and, for $\delta = 1$, i.e., $s = 2$, the system shows inactive phase. Moreover, the system shows continuous phase transition dynamics for increasing δ parameter. Therefore, it is possible to capture the continuous nature of phase transition after introducing correlated s -skewed updating scheme. That is, if we change the updating scheme to get the microscopic view, it is possible to observe the continuous nature of abrupt phase change. However, we are still open with many questions on correlated s -skewed updating scheme which depicts the future direction of this study.

3. Next, we discuss a special case following the above discussion where the ECA system shows phase transition for only $s_c = 2$. That is, the atomicity property plays the important rule for phase transition dynamics. Here, Fig. 11 depicts the space-time diagram of ECA 26 where the system shows active phase for $s \in [2, n]$ (i.e., the system without atomicity property); however, the system depicts inactive N class for $s = 1$ (i.e., the system with atomicity property). Here, the two-dimensional density surface reflects a “*surface with phase transition for $s_c = 2$* ”, see Fig. 11. Observe that, here, the quantitative indicator d_p is big and the others (d_q and d_r) are small; therefore, the density surface shows class B dynamics. The same is also true for activity surface. According to Table 4, ECA 58, 90 and 122 also depict similar phase transition dynamics. Apart from the phase transition dynamics, here, ECA 26 also reflects strange *class transition* dynamics.

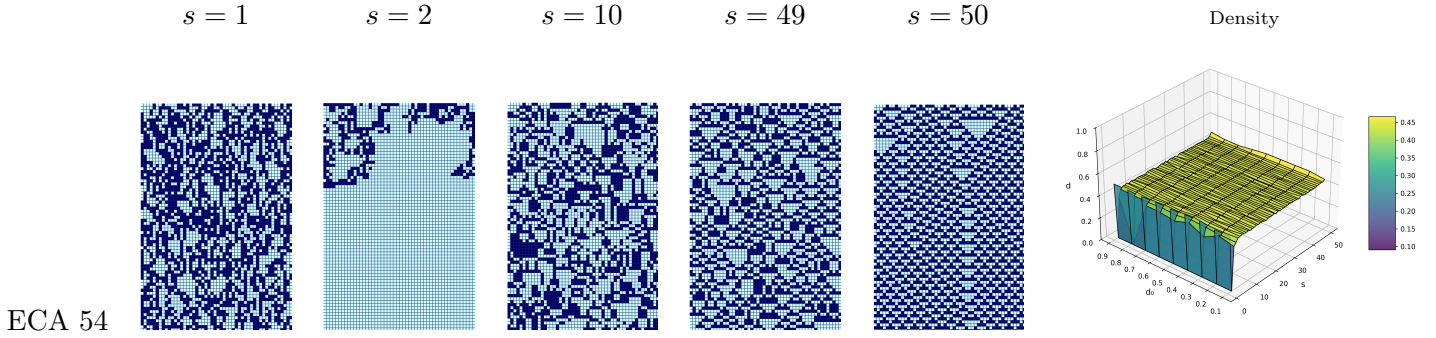


Fig. 12. Phase transition dynamics of ECA 54 under s -skewed updating scheme. Here, ECA 54 depicts a *phase transition surface with V structure* (density surface).

Observe that, ECA 26 depicts locally chaotic dynamics for synchronous update; $s = n = 50$ in Fig. 11. However, if we introduce s -skewed perturbation, the system reflects chaotic dynamics. That is, ECA 26 shows chaotic dynamics for $s = 25, 40$ in Fig. 11. Therefore, a locally chaotic (relatively simple) elementary CA system moves towards chaos with the effect of s -skewed perturbation. We discuss this class transition dynamics in the next section (in details).

4. Lastly, we discuss the situation where the cellular system changes its phase multiple time for changing perturbation rate. For example, Fig. 12 shows the space-time diagram of ECA 54, where the system shows active dynamics for $s = 1$. Next, the system depicts inactive dynamics for $s = 2$. Again, the system is capable to reflect active dynamics for $s = 10, 40, 50$ in Fig. 12. Here, the two-dimensional density surface depicts a “*phase transition surface with V structure*”, see Fig. 12. According to Table 4, ECA 22 ($n \in 2\mathbb{N}$) and 150 also depict similar phase transition dynamics. Specifically, for all of these rules, the two critical value for phase transition are $s_c = 3$ and $s_c = 2$. Therefore, traditional skewed asynchronous updating scheme ($s = 2$) [Roy et al., 2024b] and fully asynchronous update with atomicity property [Sethi et al., 2016] both plays an important rule in this situation. Moreover, the quantitative information indicators d_p and d_r are big, and, d_q is small, i.e., class D .

To sum up, here, the s -skewed asynchronous system reports following variety of phase transition dynamics:

- *surface with phase transition for $2 > s_c < n$;*
- \sqcup *surface with phase transition for $s_c = 2$ and $s_c = n$;*
- *surface with phase transition for $s_c = 2$; and*
- *phase transition surface with V structure (with multiple critical values).*

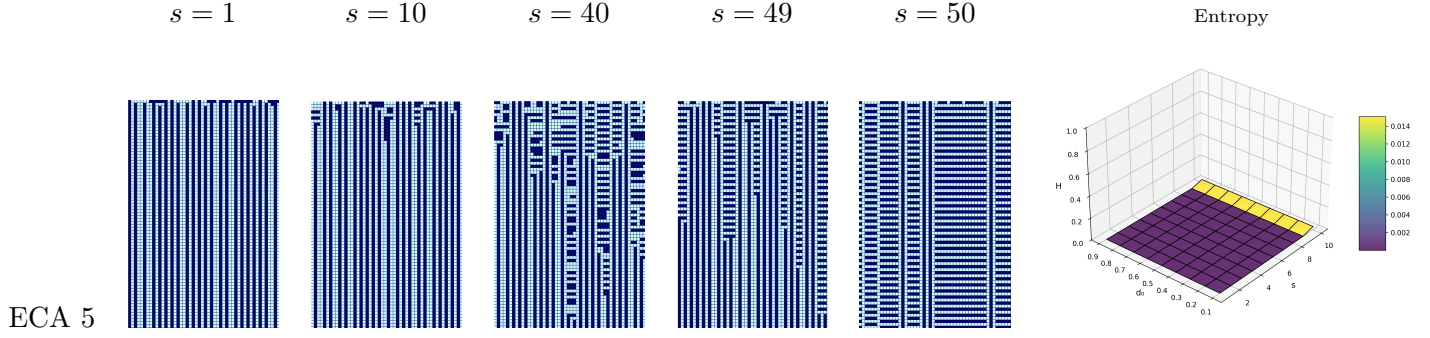
Moreover, according to the results, the presence and absence of atomicity property plays critical role in phase transition dynamics for many ECA rules.

4.4. Class transition Dynamics of s -skewed system

In this section, we discuss the *class transition* dynamics of s -skewed asynchronous system where the system shows different class dynamics following the Li-Packard's [Li & Packard, 1990] classification for different skewed perturbation rates s . Here again, we denote the critical perturbation rate for class transition as s_c . Following this, the class transition dynamics reports the following situation - $\mathbb{C}(R, u) \neq \mathbb{C}(R, v)$ where $u \in [1, s_c - 1]$, $v \in [s_c, n]$, $R \in$ class transition. Moreover, to distinguish class transition from phase transition, here, $\mathbb{C}(R, s) \neq \mathbb{N}$ for $s \in [1, n]$. Here again, if the s -skewed system changes the class dynamics multiple time for the progressive change in perturbation rate s , then we get multiple critical value. In this section, to capture the quantitative class transition dynamics, we focus on two-dimensional entropy surface. Table 5 reports the 31 minimal rules of class transition class along with their class of two-dimensional surface. Here, s -skewed asynchronous system depict following categories of class transition dynamics.

Table 5. ECA rules of class transition class along with their class of two-dimensional surface under s -skewed updating scheme.

$1_{A,B,C}$	$3_{A,A,C}$	$5_{A,B,A}$	$7_{A,C,C}$	$9_{A,A,C}$	$11_{A,B,C}$	$14_{A,B,A} (n \in 2\mathbb{N})$	$15_{A,B,A} (n \in 2\mathbb{N})$	$19_{A,A,C}$
$22_{B,B,C} (n \in 2\mathbb{N} + 1)$	$23_{A,A,C}$	$25_{A,A,C}$	$27_{A,A,C}$	$30_{A,A,C}$	$33_{A,A,C}$	$35_{A,A,C}$	$37_{A,B,C}$	$41_{A,A,C}$
$43_{A,B,C}$	$45_{A,A,C}$	$46_{D,B,A}$	$51_{A,A,D}$	$57_{A,B,C}$	$60_{A,A,C}$	$62_{A,A,C}$	$73_{B,B,C}$	$94_{A,B,A}$
$105_{A,D,D}$	$108_{D,B,C}$	$129_{A,A,C}$	$137_{A,A,C}$					

Fig. 13. Abrupt Class transition of ECA 5 under s -skewed updating scheme where $\mathbb{C}_o(5) = \text{periodic} \rightsquigarrow \text{fixed point}$. Here, the two-dimensional entropy surface shows flat surface.

1. First we discuss the situation where the system depict abrupt class transition with the effect of s -skewed perturbation. For example, Fig. 13 depicts the space-time dynamics of ECA 5 where the system shows *periodic* dynamics for traditional environment, i.e. $s = n$. However, if we introduce small amount of perturbation, the system shows *Fixed point* dynamics. Moreover, this *Fixed point* dynamics remains stable for increasing perturbation rate. Therefore, $\mathbb{C}(5, n) = P \neq \mathbb{C}(5, s) = FP$ where $s \in [1, n - 1]$. Therefore, ECA 5 shows an abrupt class transition from *periodic* to *fixed point*. Following this, we denote the overall dynamics of ECA 5 under s -skewed environment as $\mathbb{C}_o(5) = \text{periodic} \rightsquigarrow \text{fixed point}$. Fig. 13 also reports the quantitative two-dimensional entropy surface which reports (almost) *flat surface* or class A. Therefore, it is not possible to identify this class transition dynamics following only quantitative information. Here, the qualitative space-time diagram (Wolfram's approach [Wolfram, 1994]) helps us to identify this class transition dynamics. In this ECA system, ECA 14 ($n \in 2\mathbb{N}$), 15 ($n \in 2\mathbb{N}$) and 94 also depict abrupt *periodic* \rightsquigarrow *fixed point* class transition dynamics. On a contrary, ECA 46 depicts the opposite abrupt *fixed point* \rightsquigarrow *periodic* class transition dynamics.
2. Next, we discuss ECA 3 where the system shows *periodic* dynamics for traditional environment, i.e., $s = n$, see Fig. 14(a). Hereafter, if we introduce s -skewed perturbation, the system shows *kind of cluster* dynamics, i.e., in the space-time diagram, there are consecutive 1s (similar 0s). In other words, there exists less number of isolated 1 and 0, for evidence see Fig. 14(a) for $s = 10, 40$. Moreover, if we increase the perturbation rate s , the size of the cluster increases, see the difference between $s = 10$ and $s = 40$ in Fig. 14(a). Further, if we increase the perturbation rate s more, the system shows *noisy* class dynamics, see Fig. 14(a) for $s = 1, 2$. Here, we introduce two new class dynamics *cluster* and *noisy*. For the noisy class, the space-time diagrams show no evidence of pattern, i.e., random on/off of isolated 0 and 1. Therefore, the overall dynamics of ECA 3 reports $\mathbb{C}_o(3) = \text{periodic} \rightsquigarrow \text{cluster} \rightsquigarrow \text{noisy}$. Obviously, the dynamics of periodic class is more stable than the cluster and noisy class. Therefore, the two-dimensional entropy surface shows a *surface showing a class transition at $s_c < 1$* . Moreover, this class change is continuous in nature. Here, quantitative information indicator H_r is high. In the ECA system, rules 1, 9, 11, 19, 25, 27, 33, 35, 43 and 51 also depict similar dynamics, i.e., *periodic* \rightsquigarrow *cluster* \rightsquigarrow *noisy*. Now, we revisit the two-dimensional entropy surface of ECA 3. Observe that (in Fig. 14(a)), the surface shows flatness after the class transition. However, that is true for all these above ECA rules. For example, Fig. 15 depicts the space-time diagram of ECA 51 which depicts $\mathbb{C}_o(51) = \text{periodic} \rightsquigarrow \text{cluster} \rightsquigarrow \text{noisy}$. However, here, the two-dimensional entropy surface shows a *surface showing a class transition at $s_c < 1$ and quasi-flatness elsewhere*.

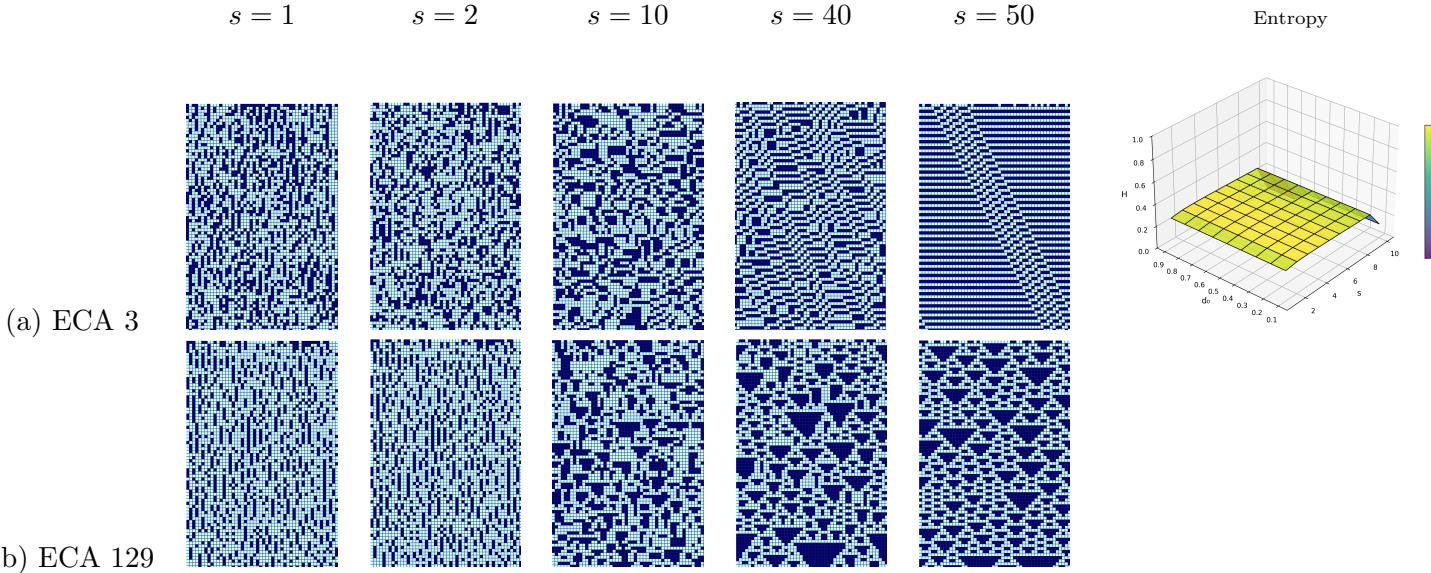


Fig. 14. Class transition dynamics of ECA 3 and 129 under s -skewed updating scheme where $\mathbb{C}_o(3) = \text{periodic} \rightsquigarrow \text{cluster} \rightsquigarrow \text{noisy}$ and $\mathbb{C}_o(3) = \text{chaotic} \rightsquigarrow \text{cluster} \rightsquigarrow \text{noisy}$. Here, the two-dimensional entropy surface shows a *surface showing a class transition at $s_c < 1$* .

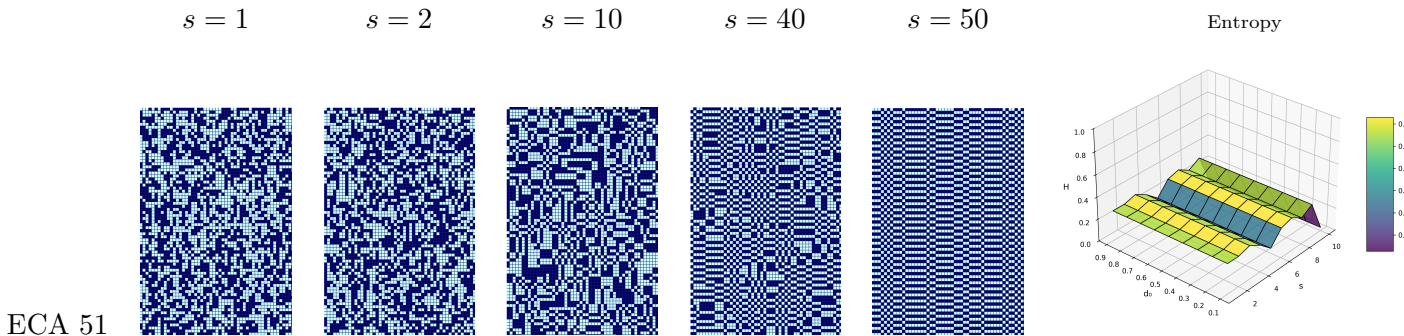


Fig. 15. Class transition dynamics of ECA 51 under s -skewed updating scheme where $\mathbb{C}_o(51) = \text{periodic} \rightsquigarrow \text{cluster} \rightsquigarrow \text{noisy}$. Here, the two-dimensional entropy surface shows a *surface showing a class transition at $s_c < 1$ and quasi-flatness elsewhere*.

In a similar direction, ECA rules 41, 129 and 137 show following class transition dynamics: *chaotic \rightsquigarrow cluster \rightsquigarrow noisy*. Here, the two-dimensional entropy surface also depict similar dynamics. For example, Fig. 14(b) depicts the space-time dynamics for ECA 129. Here, ECA 60 and 105 ($n \notin 4\mathbb{N}$) depict *chaotic \rightsquigarrow noisy*; and ECA 108 shows *periodic \rightsquigarrow noisy* dynamics (with similar entropy surface).

3. Next, we discuss ECA 7 where the divisibility of CA size by two plays an important role [Roy *et al.*, 2024a]. Let us first consider $n \in 2\mathbb{N}$ in Fig. 16(a). Fig. 16(a) depicts the class transition for ECA 7 where the ECA system shows the periodic dynamics for traditional synchronous update, i.e., $s = n = 50$. Hereafter, the system depicts the cluster dynamics for increasing s -skewed perturbation rate, see Fig. 16(a) for $s = 10, 40$. Lastly, for high perturbation rate, ECA 7 shows fixed point dynamics, see Fig. 16(a) for $s = 1, 2$. Therefore, we write $\mathbb{C}_o(7) = \text{periodic} \rightsquigarrow \text{cluster} \rightsquigarrow \text{fixed point}$ for $n \in 2\mathbb{N}$. Here, the two-dimensional entropy surface reports a \cap *surface with class transition*, see Fig. 16(a). For $n \in 2\mathbb{N} + 1$, ECA 7 depicts $\mathbb{C}_o(7) = \text{periodic} \rightsquigarrow \text{cluster} \rightsquigarrow \text{periodic}$, see Fig. 16(b). In this cellular system, ECA 23 and 37 also depict same dynamics. Moreover, in the similar direction, ECA rules 22 ($n \in 2\mathbb{N} + 1$), 30 and 45 depict the following class transition dynamics depending on the CA size: *chaotic \rightsquigarrow cluster \rightsquigarrow fixed point/periodic*.

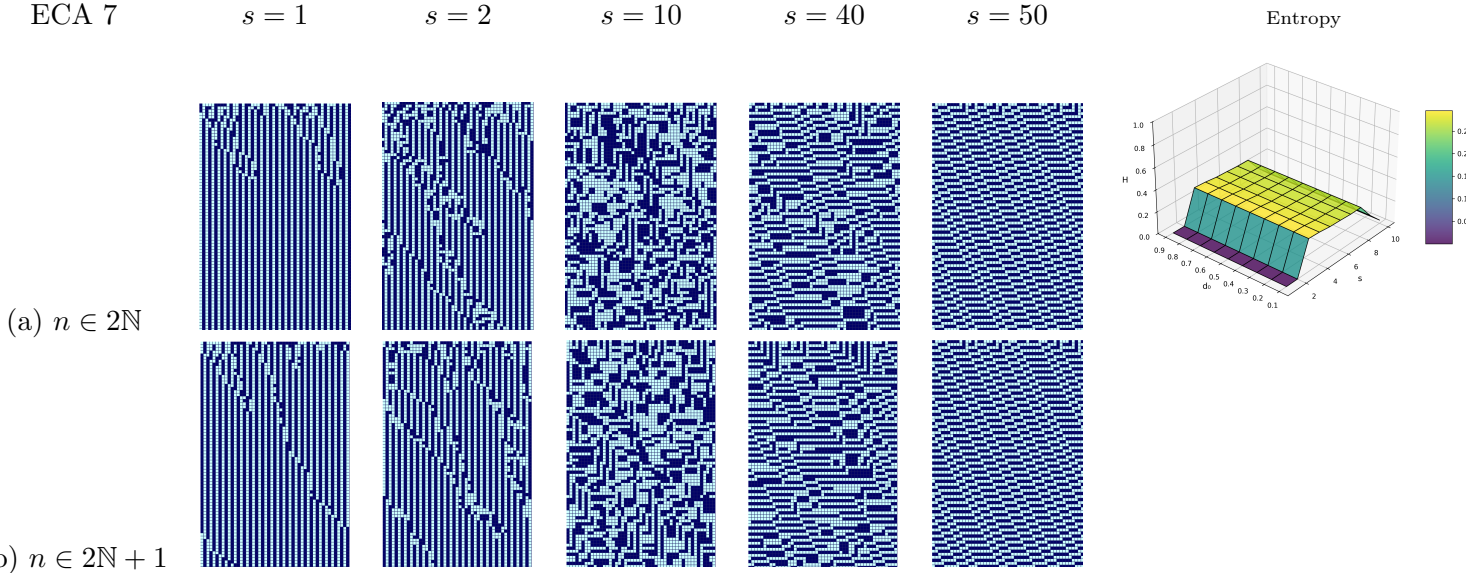


Fig. 16. Class transition dynamics of ECA 7 under s -skewed updating scheme where $\mathbb{C}_o(7) = \text{periodic} \rightsquigarrow \text{cluster} \rightsquigarrow \text{fixed point}$ for $n \in 2\mathbb{N}$, and $\mathbb{C}_o(7) = \text{periodic} \rightsquigarrow \text{cluster} \rightsquigarrow \text{periodic}$ for $n \in 2\mathbb{N} + 1$. Here, the two-dimensional entropy surface shows a \cap surface with class transition.

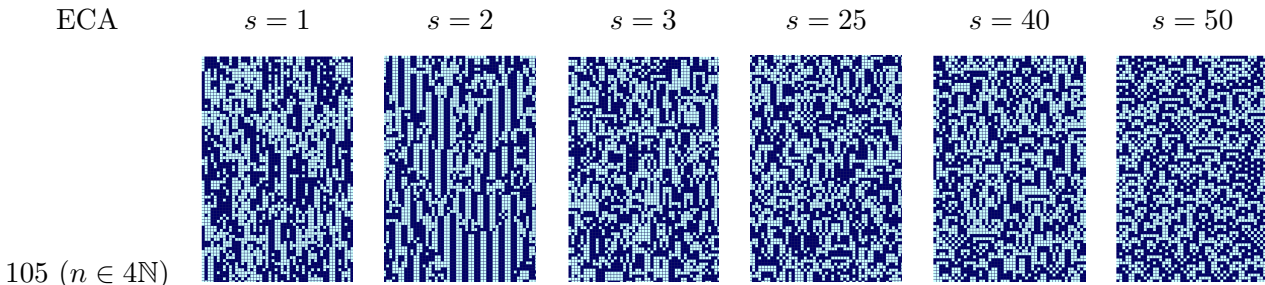


Fig. 17. Class transition dynamics of ECA 105 ($n \in 4\mathbb{N}$) under s -skewed updating scheme.

Apart from these above situations, we discuss ECA 105 ($n \in 4\mathbb{N}$, i.e., CA size is divisible by 4) where the atomicity property [Sethi *et al.*, 2016] and traditional skewed update ($s = 2$) [Roy *et al.*, 2024b] plays an important role in the class transition dynamics. Here, Fig. 17 depicts the space-time diagram for ECA 105 ($n \in 4\mathbb{N}$). Observe that, the system shows *noisy* dynamics with the presence of atomicity property ($s = 1$). Hereafter, in the absence of atomicity property, ECA 105 depicts *fixed point* dynamics. Then in the absence of traditional skewed update ($s = 3$), ECA 105 again depicts *noisy* dynamics. Hereafter, with the decreasing perturbation rate, the system moves from *noisy* to *chaotic*. Therefore, $\mathbb{C}_o(105) = \text{chaotic} \rightsquigarrow \text{noisy} \rightsquigarrow \text{fixed point} \rightsquigarrow \text{noisy}$ for $n \in 4\mathbb{N}$. To sum up, here, the s -skewed system shows following two-dimensional entropy surface to capture the class transition dynamics.

- *flat surface* where it is not possible to identify class transition following quantitative information;
- *surface showing a class transition at $s_c < 1$* where the rest of the surface after class transition shows flatness;
- *surface showing a class transition at $s_c < 1$ and quasi-flatness elsewhere*; and
- \cap surface with class transition.

Apart from these, locally chaotic ECA 26 displays the most interesting class transition dynamics where the simple locally chaotic system is able to show chaotic dynamics with the effect of s -skewed perturbation (see Fig. 11). However, the same is not true for another locally chaotic rule ECA 73 which moves from

locally chaotic to noisy with the effect of s -skewed perturbation.

5. Conclusion

To sum up, here, we classify the ECA system into four classes according to the qualitative and quantitative behaviour under s -skewed updating scheme. Here, 31 ECA rules show strong resistance against s -skewed perturbation, i.e., their qualitative and quantitative dynamics remain same after introducing s -skewed perturbation. However, the rest of the ECA system shows variety of phase transition and class transition dynamics with the effect of s -skewed perturbation. In terms of phase transition dynamics, this ECA system shows following behaviour:

1. 16 ECA rules show *discontinuity surface at $s_c = n$* , where the system depicts abrupt phase transition, i.e., discontinuity class. For these rules, the system shows massive change after introducing small ($s = n - 1$) amount of s -skewed perturbation.
2. ECA 18, 50, 106, 146 and **178** depict a *surface with phase transition for $2 > s_c < n$* .
3. ECA 6, 38, 134 report a \sqcup *surface with phase transition for $s_c = 2$ and $s_c = n$* .
4. ECA 26, 58, **90**, and **122** show a *surface with phase transition for $s_c = 2$* .
5. ECA **22** ($n \in 2\mathbb{N}$), **54**, **150** report a *phase transition surface with \vee structure* (with multiple critical value).

In the literature, Fates [Bouré *et al.*, 2012] have identified that ECA 6, 18, 26, 38, 50, 58, 106, 134 and 146 show phase transition dynamics for α asynchronous updating scheme. Recall that, in the alpha asynchronous updating scheme, each cell is updated with probability α and not updated with probability $(1 - \alpha)$ which captures the notion of uncontrolled phenomenon. Here, all these rules also show phase transition dynamics under s -skewed updating scheme. Additionally, ECA 22 ($n \in 2\mathbb{N}$), 54, 90, 122, 150 and 178 depict phase transition dynamics under s -skewed environment which is not true for α asynchronous updating scheme (in bold). For evidence, Fig. 18 depicts the space-time diagram of ECA 22 ($n \in 2\mathbb{N}$) and 54 under s -skewed and α asynchronous updating schemes. Here, the reason behind these different signature behaviour (between s -skewed and α asynchronous) indicates towards importance of atomicity property [Sethi *et al.*, 2016] and traditional skewed ($s = 2$) situation [Roy *et al.*, 2024b]. However, we are still open to this question. In a different direction, to understand the abrupt phase transition dynamics under s -skewed update, here, we introduce the notion *correlated s-skewed* updating scheme which is able to capture continuous nature of phase transition dynamics (microscopic view). However, in this article, we have not fully explored the correlated s -skewed updating scheme, which is directed towards the future direction of this study. Apart from the phase transition dynamics, here, the s -skewed system reports following various kind of class transition dynamics: *periodic \rightsquigarrow fixed point*; *periodic/chaotic \rightsquigarrow cluster \rightsquigarrow noisy*; *periodic/chaotic \rightsquigarrow noisy*; and *periodic \rightsquigarrow cluster \rightsquigarrow fixed point/periodic*. In the class transition dynamics, ECA 26 depicts a peculiar class change from *locally chaotic* to *chaotic* with the effect of s -skewed perturbation. Moreover, divisibility of CA size by 2, 3 and 4 plays crucial role in both class transition and phase transition dynamics. However, the direction of this study is limited to only qualitative and quantitative experimental approaches. What can be said about the theoretical reason behind this phase and class transition dynamics is still open to us, and it depicts the future direction.

Acknowledgements

The authors are grateful to Prof. Nazim Fates, Prof. Sukanta Das and Subrata Paul for enlightening discussions on this topic.

References

- Bouré, O., Fates, N. & Chevrier, V. [2012] “Probing robustness of cellular automata through variations of asynchronous updating,” **11**, 553564.
- Bouré, O., Fates, N. A. & Chevrier, V. [2011] “Robustness of Cellular Automata in the Light of Asynchronous Information Transmission,” *10th International Conference on Unconventional Computing*,

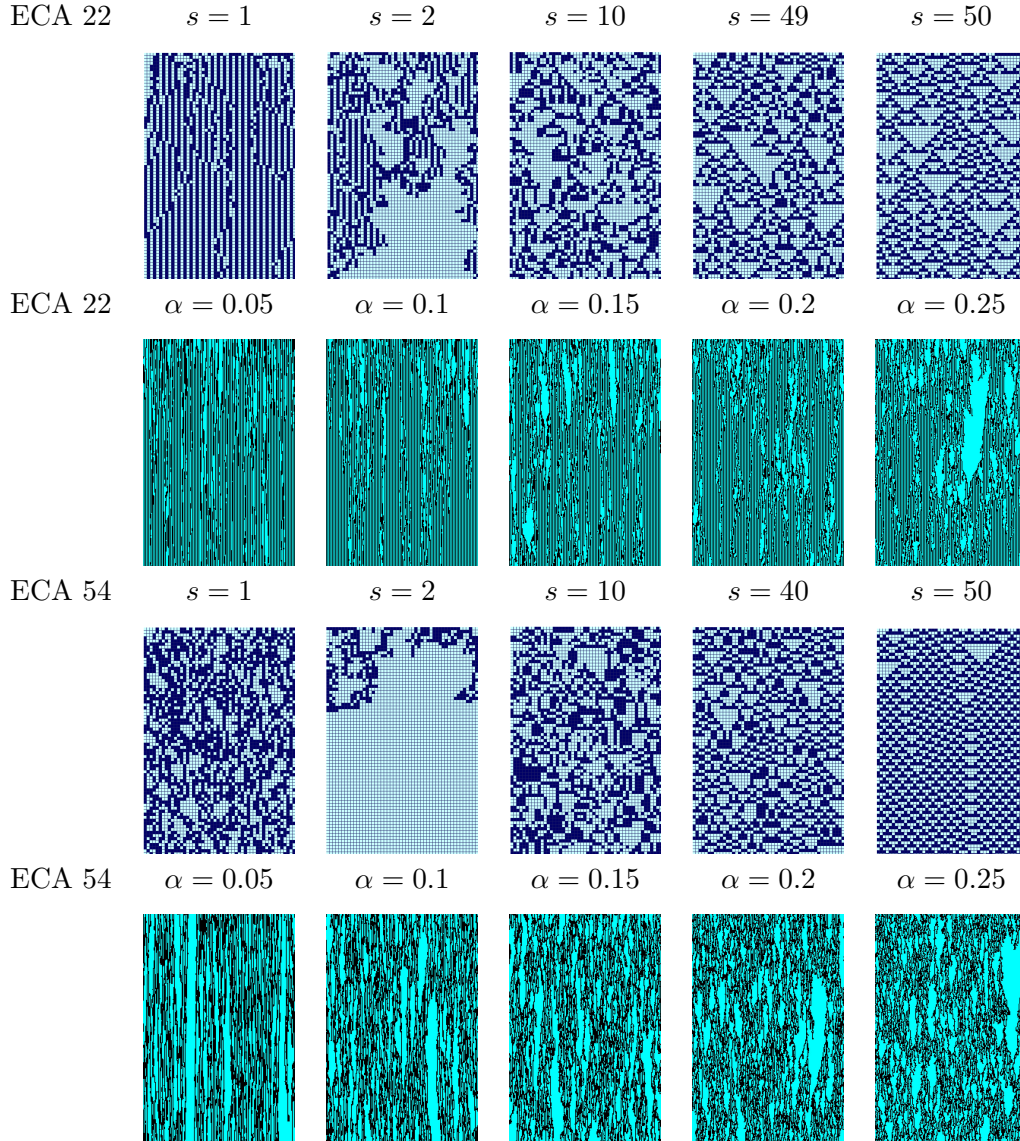


Fig. 18. Dynamics of ECA 22 ($n \in 2N$) and 54 under s -skewed and α asynchronous updating schemes. Here, s -skewed system depicts phase transition for both of these rules which is not true for α asynchronous system.

- eds. Calude, C. S., Kari, J., Petre, I. & Rozenberg, G. (Springer, Turku, Finland), pp. 52–63, doi: 10.1007/978-3-642-21341-0\11, URL <https://inria.hal.science/inria-00563904>.
- Cori, R., Metivier, Y. & Zielonka, W. [1993] “Asynchronous mappings and asynchronous cellular automata,” *Information and Computation* **106**, 159–202.
- Fatès, N. [2014] “Guided tour of asynchronous cellular automata,” *Journal of Cellular Automata* **9**, 387–416.
- Fatès, N. [2024] “Asynchronous cellular systems that solve the parity problem,” *Cellular Automata and Discrete Complex Systems*, eds. Gadouleau, M. & Castillo-Ramirez, A. (Springer Nature Switzerland, Cham), ISBN 978-3-031-65887-7, pp. 133–145.
- Fates, N. & Morvan, M. [2005] “An experimental study of robustness to asynchronism for elementary cellular automata,” *Complex Systems* **16**, 1–17.
- Fates, N., Thierry, E., Morvan, M. & Schabanel, N. [2006] “Fully asynchronous behavior of double-quiescent elementary cellular automata,” *Theoretical Computer Science* **362**, 1 – 16.
- Fates, N. [2003] “Experimental study of Elementary Cellular Automata dynamics using the density pa-

- rameter,” *Discrete Mathematics & Theoretical Computer Science DMTCS Proceedings vol. AB, Discrete Models for Complex Systems (DMCS’03)*, doi:10.46298/dmtcs.2304, URL <https://dmtcs.episciences.org/2304>.
- Kamilya, S. & Das, S. [2019] “A study of chaos in non-uniform cellular automata,” *Communications in Nonlinear Science and Numerical Simulation* **76**, 116–131, doi:<https://doi.org/10.1016/j.cnsns.2019.04.020>, URL <https://www.sciencedirect.com/science/article/pii/S1007570419301315>.
- Lei, Q., Lee, J., Huang, X. & Kawasaki, S. [2021] “Entropy-based classification of elementary cellular automata under asynchronous updating: An experimental study,” *Entropy* **23**, doi:10.3390/e23020209, URL <https://www.mdpi.com/1099-4300/23/2/209>.
- Li, W. & Packard, N. [1990] “The structure of the elementary cellular automata rule space,” *Complex Systems* **4**, 281–297.
- Martínez, G. J., Adamatzky, A. & Alonso-Sanz, R. [2013] “Designing complex dynamics in cellular automata with memory,” *International Journal of Bifurcation and Chaos* **23**, 1330035, doi: 10.1142/S0218127413300358.
- Martinez, G. [2013] “A note on elementary cellular automata classification,” *Journal of Cellular Automata* **8**, 233–259.
- Ninagawa, S., Adamatzky, A. & Alonso-Sanz, R. [2014] “Phase transition in elementary cellular automata with memory,” *International Journal of Bifurcation and Chaos* **24**, 1450116, doi:10.1142/S0218127414501168.
- Roy, S. [2019] “A study on delay-sensitive cellular automata,” *Physica A: Statistical Mechanics and its Applications* **515**, 600–616.
- Roy, S. [2021] “Distributed computing on cellular automata with applications to societal problems,” PhD thesis, Indian Institute of Engineering Science and Technology, Shibpur.
- Roy, S., Fats, N. & Das, S. [2024a] “Reversibility of elementary cellular automata with fully asynchronous updating: An analysis of the rules with partial recurrence,” *Theoretical Computer Science* **1011**, 114721, doi:<https://doi.org/10.1016/j.tcs.2024.114721>, URL <https://www.sciencedirect.com/science/article/pii/S0304397524003384>.
- Roy, S., Gautam, V. K. & Das, S. [2024b] “A note on skew-asynchronous cellular automata,” *Cellular Automata and Discrete Complex Systems*, eds. Gadouleau, M. & Castillo-Ramirez, A. (Springer Nature Switzerland, Cham), ISBN 978-3-031-65887-7, pp. 146–158.
- Roy, S., Paul, S. & Das, S. [2022] “Temporally stochastic cellular automata: Classes and dynamics,” *International Journal of Bifurcation and Chaos* **32**, 2230029, doi:10.1142/S0218127422300294.
- Salvi, S., Shelat, S., Adak, S. & Roy, S. [2025] “The “distributed ghost” with independence - a study on computational ability of skewed asynchronous cellular automata,” *Proceedings of International Conference on Complex Systems Modeling, Analysis & Applications*.
- Sethi, B., Roy, S. & Das, S. [2016] “Asynchronous cellular automata and pattern classification,” *Complexity* **21**, 370–386, doi:<https://doi.org/10.1002/cplx.21749>, URL <https://onlinelibrary.wiley.com/doi/abs/10.1002/cplx.21749>.
- Vispoel, M., Daly, A. J. & Baetens, J. M. [2022] “Progress, gaps and obstacles in the classification of cellular automata,” *Physica D: Nonlinear Phenomena* **432**, 133074, doi:<https://doi.org/10.1016/j.physd.2021.133074>, URL <https://www.sciencedirect.com/science/article/pii/S0167278921002311>.
- Wolfram, S. [1994] “Cellular automata and complexity: Collected papers (1st ed.),” *CRC Press*.